Flexible cell designs for simultaneous electrochemical electron spin resonance measurements with a coaxial microwave cavity

ARTICLE *in* REVIEW OF SCIENTIFIC INSTRUMENTS · OCTOBER 2000

Impact Factor: 1.61 · DOI: 10.1063/1.1289676

2 AUTHORS:

Lin Zhuang
Wuhan University
90 PUBLICATIONS **3,191** CITATIONS
SEE PROFILE

Juntao Lu
Wuhan University
93 PUBLICATIONS **2,483** CITATIONS
SEE PROFILE

Flexible cell designs for simultaneous electrochemical electron spin resonance measurements with a coaxial microwave cavity

Lin Zhuang[a] and Juntao Lu
Department of Chemistry, Wuhan University, Wuhan 430072, People's Republic of China

(Received 24 March 2000; accepted for publication 1 July 2000)

New cell designs of coaxial microwave cavity type are reported for simultaneous electrochemical electron spin resonance measurements. Adjustable metallic shields are introduced so that the working electrode can be much shorter than the full height of the cavity. Besides the traditional helical electrode, the working electrode can be cylinders made from metallic plates, meshes, or even composite materials. The counter electrode can be placed either inside or outside the cavity. These features make the new designs more flexible than those previously reported. The impacts of eddy currents due to the magnetic-field modulation are examined and discussed. With a nonperforated cylindrical electrode, this cell can be used to determine the standard potential and the number of electrons transferred in electrode reactions involving radicals. Other possible applications are also briefed. © *2000 American Institute of Physics.* [S0034-6748(00)01410-6]

I. INTRODUCTION

Since its early stage of development, electron spin resonance (ESR) has been combined with electrochemistry. Simultaneous electrochemical-ESR (SEESR) measurements can be used for different purposes and, therefore, are of interdisciplinary interest. Some researchers may use electrochemistry as a unique tool for *in situ* generation of radicals to study the ESR behaviors of radicals or to analyze the structure of the radicals. Electrochemists may use ESR to detect and study the paramagnetic species involved in electrode reactions. These paramagnetic species may be the intermediate, product, or catalyst in an electrode reaction. The charge carrier electrons in conducting polymers and lithium intercalation carbons can also be studied by SEESR measurements.

The cell design is a key to success in SEESR measurements. A good cell design should be able to meet the conditions required for both normal ESR measurements and electrochemical operations. However, the conditions required by the two sides are often in conflict to some extent. On one hand, a highly conductive electrolyte solution favored by electrochemical operations inevitably tends to cause serious dielectric loss to the ESR cavity. On the other hand, in order for the ESR measurement to be conducted normally, the volume of the SEESR cell is severely limited and the cell shape must meet some special requests. For a rectangular ESR cavity, the available space for the SEESR cell is about 1 cm wide with the maximum length equal to the height of the cavity and a thickness no more than 0.5 mm. For a cylindrical cavity, the effective volume of the cell is confined in a cylindrical space of 1–2 mm diameter around the axis of the cavity. Consequently, most of the reported cell designs fall into two basic categories, i.e., flat cells and capillary cells, to fit the two cavities, respectively.

A properly designed SEESR cell should be not only able to produce reliable data but also easy to handle. A variety of cell designs have been reported in the literature and a few reviews are available.[1–3] Each cell design has its merits and shortcomings and is applicable to a wider or narrower range of experimental parameters, such as the dielectric constant of the solvent, the concentration of paramagnetic species, the required precision of potential control over the working electrode, the duration of undistorted semifinite diffusion mode, the time constant for exhausting electrolysis, etc. In this article, we report new cell designs based on the coaxial microwave cavity concept with an emphasis on improving the flexibility and widening applicability.

The first cell design based on the concept of coaxial microwave cavity was reported by Allendoerfer and co-workers.[4] In their design the working electrode is a finely wound metal helix fitted snugly against the inner wall of an ESR sample tube of 6 mm inner diameter. The length of the helix is somewhat longer than the height of the cylindrical cavity (about 4.4 cm for *X*-band microwave). The counter electrode is located in the center of the helix while the Luggin capillary for the reference electrode is placed close to the inner surface of the helix. The ESR observable space is confined to the volume between the metal helix and the inner wall of the sample tube. This design has some obvious advantages. This cell can be used for a wide range of solvents with different dielectric constants, from water to organic solvents. The potential over the whole working electrode surface can be fairly uniformly controlled because of the symmetric arrangement of the electrodes; the distortion of voltammogram due to IR drop is said to be negligible (we have a comment on that point, see below); the paramagnetic species generated at the counter electrode is screened from ESR detection by the metal helix; the time for exhausting electrolysis is relatively short (about 30 s); the large surface area of the working electrode makes it advantageous in detecting short-lived radicals. The performance of the cell seems very attractive; however, the long and finely wound

[a]Author to whom correspondence should be addressed; electronic mail: lzhuang@whu.edu.cn

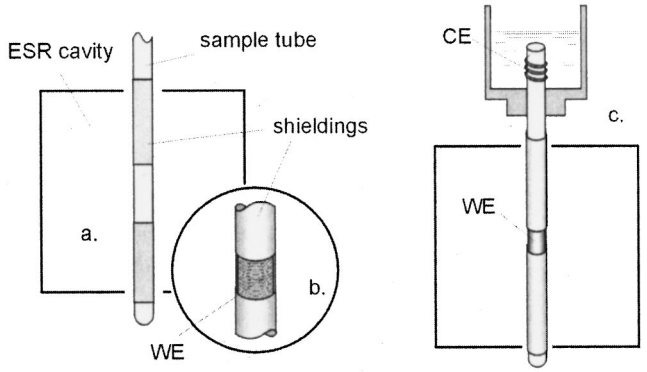

FIG. 1. The cell design. (a) The SEESR cell with adjustable shields; (b) an enlarged view of a short helical working electrode with shields; (c) the cell with the counter electrode placed outside the cavity.

helical electrode is not convenient to deal with, especially when the sample tube is thinner. For example, for a conventional ESR sample tube of 4 mm inner diameter, a 4.4 cm finely wound helix made from a metal wire of 0.3 mm diameter has over 100 turns and needs about 1.5 m of wire. It is not an easy job to make such a precisely wound helix in common laboratories. Besides, in some experiments, the electrode surface has to be cleaned mechanically. In these cases repeated unwinding and winding of the helix becomes necessary and these would easily cause a break in the wire, which is often made from noble metals and costly. The purpose of this work was to try to modify the original design so that the SEESR cell could be prepared easier and more flexible to suit a wider range of experiments.

II. EXPERIMENT

A. Cell design

In Allendoerfer's design,[4] the helix wire has two functions. In addition to being a working electrode, it prevents the bulk of the solution from microwave radiation to avoid severe dielectric loss. To be a working electrode, a full-length (the height of the ESR cavity) helix is not necessary though a long helix means a big electrode surface area favorable for the sensitivity of ESR detection. In many cases, the sensitivity is not a major concern and a much shorter helix electrode may still generate a sufficient number of radicals for ESR measurements. A shorter helical electrode is obviously easier to handle. To ensure an acceptable dielectric loss, however, the helix must be full length in Allendoerfer's design.

In the new design, a part of the shielding function of the helix is taken over by two adjustable metallic shields so that the working electrode can be much shorter. The adjustable shields are made from highly conducting metal (Ag, Cu, or Al) foils by simply wrapping the foils around the ESR sample tube and fixing them with adhesive tape [Fig. 1(a)]. Experiments show that it is important to have the outside surface of the metal shields polished bright. The two shielding cylinders can be moved up and down on demand. The gap between them is centered in the cavity. The length of the working electrode just fills the gap. In this way, a helix working electrode can be much shorter than the cavity

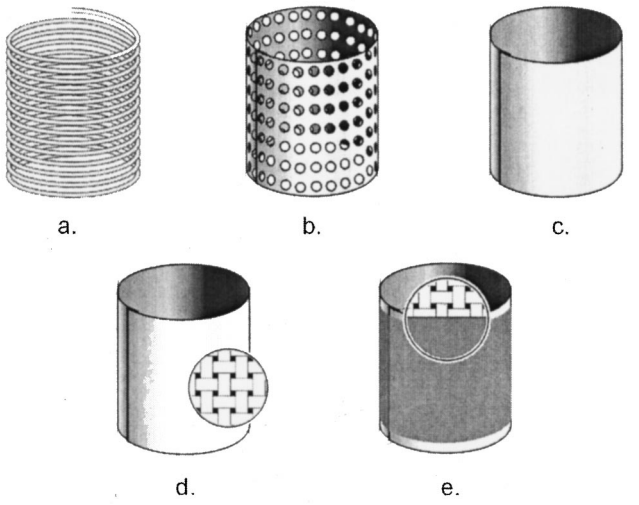

FIG. 2. Examples of the working electrode for the coaxial cavity. (a) Helix; (b) perforated cylinder; (c) nonperforated cylinder; (d) metallic mesh; (e) carbon sheet-metallic mesh composite.

height. Besides the wound metal wire, the working electrode may also be a cylinder made from different materials, such as perforated or nonperforated metal foils, metallic mesh, or even composite sheets (Fig. 2).

In most experiments reported in this article, the counter electrode was a platinized thick Pt wire located in the center of the cell along the axis. A roughened silver wire sealed in a thin Teflon tube served as an acting reference electrode. Another thin Teflon tube was inserted down to the cell bottom for purging the solution with argon.

In prolonged experiments, the product formed at the counter electrode may eventually reach the working electrode through convectional diffusion and cause interference to SEESR measurements. In these cases, the counter electrode can be moved outside the cavity as shown in Fig. 1(c). In this design, the convectional mass transport for the species formed at the counter electrode is essentially eliminated by the special configuration. If the density of the product at the counter electrode is lower than that of the bulk solution, it will rise up and float at the top of the solution; if the density is higher than that of the bulk solution, it will sink down and stay at the bottom of the upper container outside the cavity. The long distance between the counter and the working electrodes makes it practically impossible for the products to diffuse from the counter to the working electrode. Thus, the interference caused by the product at the counter electrode can be effectively avoided. This advantage is obviously obtained at the expense of the uniformity of potential distribution over the working electrode. For a given electrochemical system, the potential nonuniformity due to ohmic drop is determined by the ratio of the electrode length and the cross-section area of the electrolyte channel in contact with the electrode. In this connection, the design in Fig. 1(c) is still better than the widely cited flat cell.[5] To give an impression of the IR effects of this cell, here we present a set of cyclic voltammograms obtained with 1 mmol/l $Fe(CN)_6^{3-/4-}$ in 0.5 mol/L KCl (Fig. 3). The peak potential separations for scan rates 1, 10, 40, and 100 mV/s are approximately 40, 70, 90,

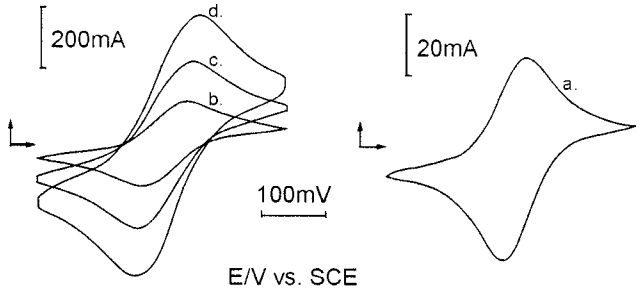

FIG. 3. Cyclic voltammograms obtained with the cell design shown in Fig. 1(c) for 1 mmol/L $Fe(CN)_6^{3-/4-}$ in 0.5 mol/L KCl at scan rates (mV/s) (a) 1, (b) 10, (c) 40, and (d) 100.

and 105 mV, respectively. The 40 mV of peak separation for the slowest scan is smaller than the typical value for a one-electron reversible system, 59 mV. This was caused by the thin layer effect, which is characteristic for all the coaxial cell designs mentioned in this article and will be discussed below in more detail.

B. Instrumentation and methods

ESR measurements were conducted on a JEOL JES-FE1XG ESR spectrometer with TE_{011} cylindrical cavity working at *X* band. A Mn(II) marker was kept in the cavity to serve as both the indicator for the *Q* factor of the cavity and the internal scale for the magnetic field. The electrochemical system consisted of a Pine AFRDE5 bipotentiostat and YEW 3036 *x-y* recorder. All experiments were performed at room temperatures. The potentials are reported with respect to SCE.

To test the effectiveness of the adjustable shields and the influence of the gap width on ESR measurements, ESR intensity was measured as a function of the gap width using an aqueous solution of 4-hydroxyl-TEMPO (2,2,6,6-tetramethyl piperidine oxyl-1, Sigma) as a sample. To demonstrate the performance of the cell, SEESR measurements were carried out using methylviologen (MV, BDH Chemicals) as a model system. Modifications in cell configuration were made in some individual applications and additional experimental details will be given in relevant sections below.

III. RESULTS AND DISCUSSION

The behaviors of the helical electrode in the presence of the adjustable shields were essentially identical to that of the full-length helical electrode as reported by Allendoerfer,[4] except for the dependence of ESR sensitivity on the gap width. Therefore, we here only report and discuss the results associated with the new features of the cell designs, including the effects of the adjustable shields and the performance of different working electrodes. Besides, eddy-current effects and the thin layer effect that were overlooked in previous articles will also be discussed.

A. The effects of the adjustable shields

Figure 4(a) shows the measured ESR intensity, I_{ESR}, as a function of the gap widths between the two shielding cylinders. The gap was centered in the ESR cavity and a full-length helix made of silver wire of 0.3 mm diameter was

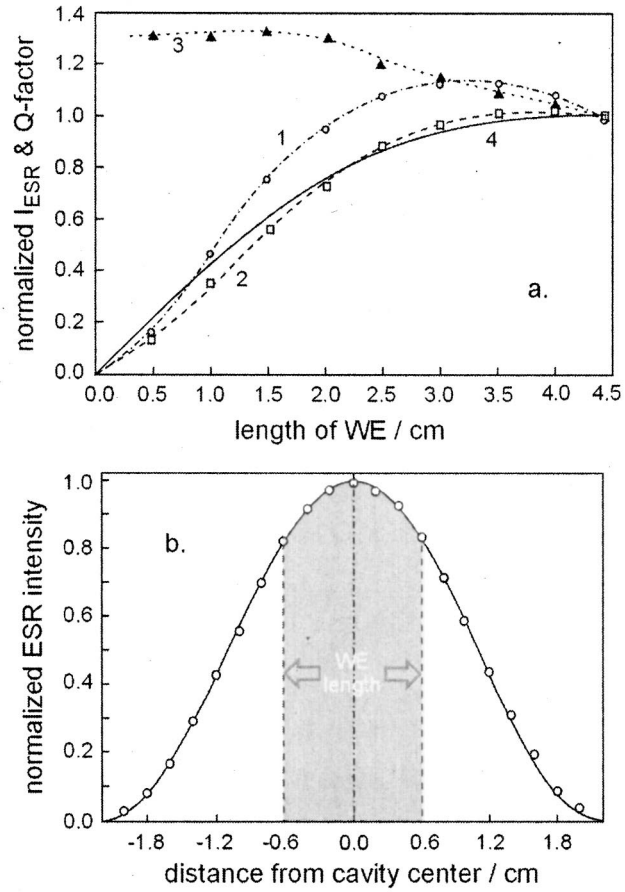

FIG. 4. Influence of gap width on ESR measurements. (a) Normalized ESR intensities and *Q* factors vs gap width: 1, measured ESR intensity; 2, ESR intensity after correction for *Q*-factor changes; 3, normalized *Q* factor; 4, ESR intensity calculated from b. (b) Normalized ESR intensity for a DPPH ring probe located at varying height in the cavity (open circles) and the theoretical curve $\cos^2(\pi x/h)$ (solid line).

snugly fitted the inside wall of a conventional ESR tube (inner diameter 4 mm) filled with an aqueous solution of 4-hydroxyl-TEMPO (~1 mmol/L). The ESR intensity obtained without the shields is used as the basis for normalization in Fig. 4(a). Curve 1 shows that the measured ESR intensity initially increases with increasing gap width then reaches a maximum located about 3/4 of the full length and finally decreases to unity.

There were three main factors influencing curve 1 in Fig. 4(a): the number of radicals radiated by the microwave, the ESR sensitivity distribution along the cavity axis, and the *Q* factor of the cavity. The *Q* factor of cavity was indicated by the ESR intensity of the Mn(II) marker and normalized with respect to the *Q* factor for the full-length gap as shown by curve 3. It is seen that the *Q* factor values for gaps smaller than 2 cm is about 30% higher than that for full-length gap (4.4 cm). After correction for the changes in *Q* factor, curve 1 becomes curve 2.

Figure 4(b) shows the normalized ESR sensitivity distribution along the axis in the cavity. The data points represent the normalized ESR signal intensity of a diphenylpicrylhydrazyl (DPPH) probe. The probe was a narrow ring (about 1 mm wide) of filter paper containing DPPH and fixed around

an empty ESR sample tube. The sample tube was then put in the cavity and brought up and down to obtain ESR signals of the probe at different locations along the axis. In all these measurements, the whole height of cavity was filled with the empty ESR tube to keep the Q factor constant. As shown in Fig. 4(b), the data points fit well the theoretical curve $\cos^2(\pi x/h)$ (the solid line) for the microwave intensity distribution in the cavity,[3] where x is the distance from the cavity center along the cavity axis and h is the height of the cavity. Curve 4 in Fig. 4(a) is the normalized integrated ESR sensitivity which is represented by the shadowed area in Fig. 4(b) for a given gap width. The reasonable agreement between curves 4 and 2 in Fig. 4(a) confirms the above mentioned main factors governing curve 1 in Fig. 4(a). The slight difference between curves 2 and 4 in Fig. 4(a) may be attributed to distortions of microwave field due to the insertion of the electrochemical cell.

It is interesting to note the favorable features of curve 1 in Fig. 4(a). The maximum at the gap width 3 cm is about 30% higher than the ESR intensity of the full-length helical electrode. One the other hand, the ESR intensity obtained with a full-length helical electrode in the original Allendoerfer's cell can now be reached by using an electrode of only half of the full length in the new design. Curve 1 in Fig. 4(a) provides a guideline to determine the gap width suitable for particular experimental conditions. When the concentration of electrochemically generated radicals is high the gap width can be made small, say only a few millimeters. If a helical electrode is to be used, it will be much easier to deal with such a short helix than a full-length one.

B. Eddy-current effects due to magnetic-field modulation

When an alternating electromagnetic field is applied to an electrically conducting object, eddy currents are induced to flow around the surface of the conductor. The eddy currents create a magnetic field that tends to cancel the change in the applied field inside the conductor, and the magnetic field of the eddy currents extends outside the conductor to perturb the external field. Although eddy-current effects are important in ESR detection, detailed discussion has hardly been seen in the literatures concerning electrochemical-ESR cell designs.[4]

In conventional ESR experiments there are two oscillating magnetic fields, the microwave magnetic field (about 9 GHz for the X band) and the magnetic-field modulation (typically 100 kHz) used for phase-sensitive signal detection. With the new cell designs, the eddy currents induced by the microwave were negligible, otherwise the Q factor would have been severely depressed. Therefore, we here only discuss the eddy-current effects due to the magnetic-field modulation. Figure 5(a) shows schematically the applied alternating modulation field B_{appl} and the induced eddy field B_{eddy}. It is seen that near the metal surface perpendicular to B_{appl} the induced field is superimposed on B_{appl} destructively while constructively near the surface tangential to B_{appl}. It follows that the effective magnetic modulation width, which is the sum of B_{appl} and B_{eddy}, is decreased in the former and increased in the latter. Since the sensitivity of ESR detection is proportional to the effective modulation width, the spatial distribution of sensitivity is expected to be uneven around the circumference. Because the larger the size of the metal the more significant the eddy-current effects, in our designs the eddy current would be most prominent when a full-length nonperforated cylindrical electrode is used. In order to examine the inhomogeneous distribution of the effective modulation width, a filter paper strip (0.5 mm wide) containing DPPH was used as a probe and fixed on a cylinder made of silver plate [Fig. 5(b)]. Figure 5(c) shows the change in ESR intensities with respect to the radial orientation of the strip measured by angle θ. It is clear that the ESR intensity reaches maximum at $\theta = 90°$ and 270° while minimum at 0° and 180°. These results are in agreement with the phenomena observed in ESR imaging measurements.[6] Using other working electrode configurations, e.g., helix or short perforated cylinder, the effect of eddy currents became less conspicuous.

The locally inhomogeneous distribution of the ESR sensitivity may seriously affect the spatial ESR imaging measurements.[7] In conventional ESR measurements, only the spatially averaged ESR intensity is recorded and, therefore, the spatial inhomogeneity of sensitivity is less prominent. However, additional ESR line broadening may be caused by the eddy field.

As is well known, in conventional ESR measurements the magnetic-field modulation width must be no more than half of the intrinsic peak-to-peak line width (ΔH_{pp}) of the ESR signal to be detected, otherwise the ESR linewidth will be abnormally broadened. This situation is shown in Fig. 6 by curve 1, which was obtained with a dilute alcohol solution of TEMPO contained in a Teflon capillary sample tube. It is seen that the spectral linewidth remains constant when the field modulation width is below 1 G. At larger modulation widths, the recorded linewidth increases with modulation widths. In the presence of eddy current, the linewidth broadening would become more prominent because in a part of the detected space the local effective modulation is larger than the value shown on the instrument panel. To demonstrate this effect, the same TEMPO solution was tested in a cell shown in Fig. 1(a) using a silver cylinder (24 mm in height) as a dummy electrode. The data thus obtained (curve 2 in Fig. 6) clearly show that the linewidth broadening is indeed more severe than in the previous case.

In conclusion, eddy-current effects do exist with metallic cylinders used in our cells. If spectral line broadening is a concern, the field modulation should be kept somewhat smaller than with conventional sample cells. For other cases where spectral broadening is not taken seriously, eddy currents do not affect measurements.

C. SEESR measurements with a perforated cylindrical electrode

To test the feasibility of the perforated cylindrical electrode as a replacement for the helical electrode, a silver cylinder was made from a piece of 0.1-mm-thick Ag plate. The

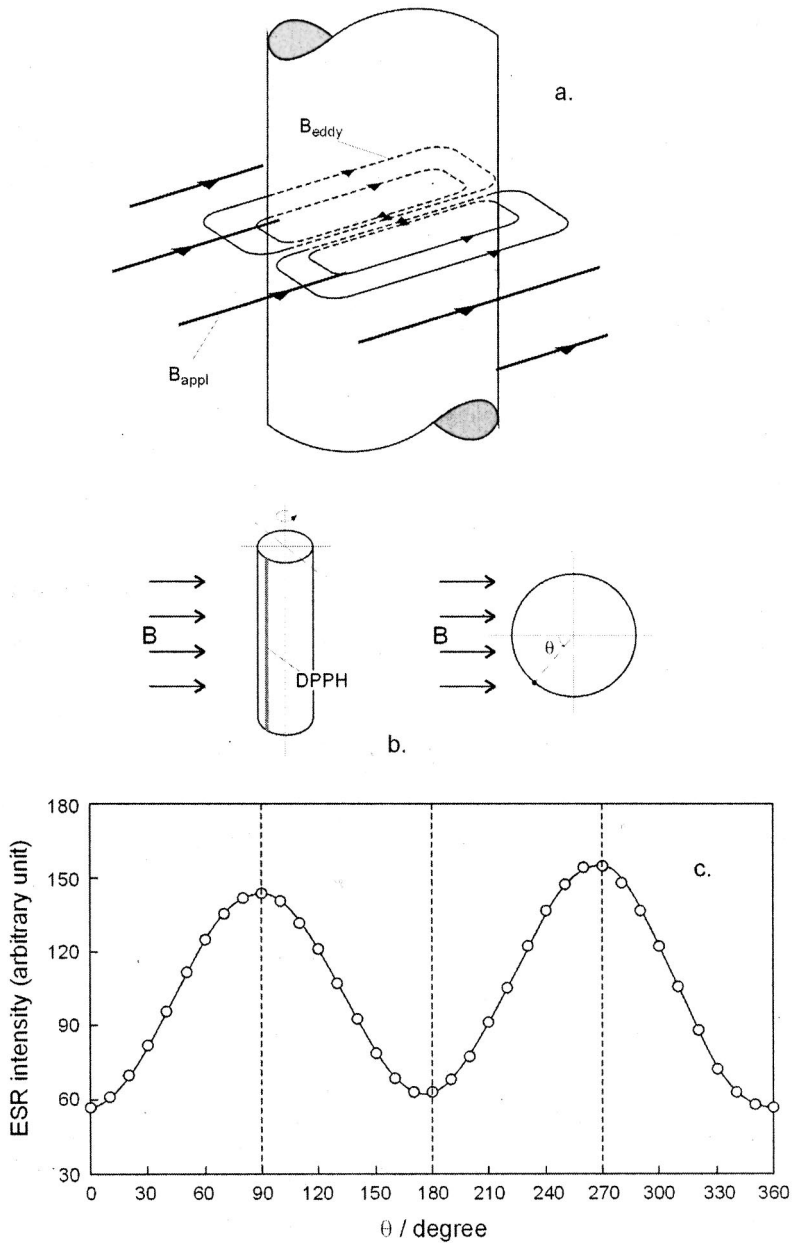

FIG. 5. Inhomogeneous distribution of ESR sensitivities caused by eddy-current effects. (a) Applied alternating modulation field B_{appl} and induced eddy field B_{eddy} in the case of coaxial microwave cavity. (b) A probing DPPH strip fixed on the cylindrical surface and at radial angle θ. (c) The change in ESR intensities with respect to θ.

holes in the plate had a diameter 0.3 mm and were arranged in about 0.9 mm×1 mm array [Fig. 2(b)].

Figure 7 shows the cyclic voltammogram for the redox reactions of methylviologen in 0.5 mol/L KCl aqueous solution and the simultaneously recorded ESR intensity at a fixed magnetic field. The two cathodic peaks correspond to the two steps of one-electron transfer

$$\text{peak I} \quad MV^{2+} + e^- \rightarrow MV^+ \tag{A}$$

$$\text{peak II} \quad MV^+ \cdot + e^- \rightarrow MV \tag{B}$$

Peak I and the corresponding anodic peak are centered round −0.69 V (versus SCE) with a peak separation of about 40 mV. This peak separation is smaller than the standard value 59 mV (25 °C) for a reversible redox couple in solution under semi-infinite diffusion conditions. The observed smaller peak separation may be attributed to the fact that the cell configuration bares to some extent the characteristics of a thin-layer cell. The space between the working electrode and the sample tube wall forms a thin layer of solution that can exchange solutes with the bulk solution only through the holes. The other side of the working electrode facing the center of the sample tube can be considered to be under semi-infinite diffusion conditions. The observed current is actually the sum of the currents generated at both sides of the working electrode. For a typical thin-layer cell, the peak separation for reversible redox couples is zero, resulting from a homogeneous consumption of the dissolved reactants in the whole thickness of the thin-layer solution. In our experiment, the situation was far from that of a typical thin-layer cell but bore some influence of the thin-layer effect. When potential scan rate was increased, this effect became less noticeable. For example, the peak separation increased to 60 mV at a scan rate of 200 mV/s.

The thin-layer effect can be regulated by changing the hole density. With increasing hole density the solution confined between the working electrode and the tube wall be-

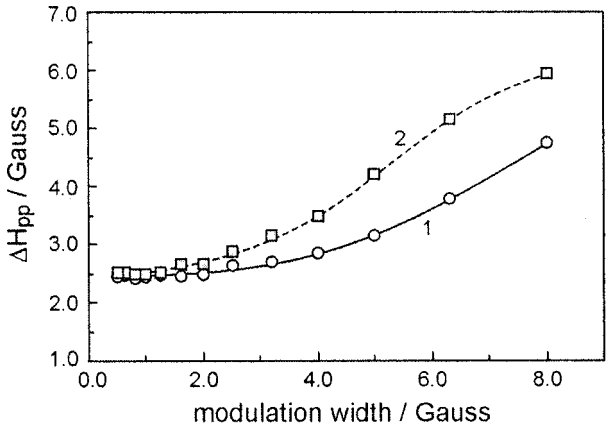

FIG. 6. Abnormal broadening in ESR linewidth. (1) In the absence and (2) in the presence of eddy-current effects.

comes less isolated from the bulk solution, resulting in a decrease in the thin-layer effect. Conversely, a decrease in hole density will make the thin-layer effects more prominent. Our experiments have proved that the thin-layer effect also exists with the helical electrode if the space between the turns is small and potential scan is slow. While the thin-layer effect may be annoying for obtaining a perfect voltammogram, it is useful in some other cases. For example, the thin-layer cell with an optical transparent electrode has been widely used for determining the standard potential and the number of electrons involved electrode reactions.[8] ESR thin-layer cell experiments can be conducted with our cylindrical working electrode and an example of this kind is given below.

D. Nonperforated cylindrical electrode used as an electrode with thin-layer solution

The optically transparent thin-layer electrode (OTTLE) is one of most popular spectroscopic methods used in electrochemistry. It features a transparent electrode in contact with a thin layer of solution. To determine the standard (or formal) potential and the number of electrons involved in redox reaction, the oxidized and reduced forms of the redox couple in the thin-layer solution reach their equilibrium values within a short time (10 s to a few minutes) on potentiostatic electrolysis and then a spectrum is taken for the given electrode potential. The cylindrical ESR electrode provides an excellent analog to OTTLE for redox couples involving radicals. In our experiment, the time of exhausting electrolysis for the thin-layer solution between the cylindrical electrode and the ESR tube was well below 30 s. As a demonstration, the data for MV^{2+}/MV^{+} couple are given in Fig. 8. The cylindrical Ag electrode used in this measurement was not perforated and had a height of 2.5 cm. The gap between the two shields was 1 cm. The upper and lower edges of the working electrode were covered with the shields to prevent the interference from the solution at the two edges. The electrode potential was controlled potentiostatically point by point, while the peak-to-peak height of a selected ESR band was taken as a measure of ESR intensity, I_{ESR}. According to the Nernst equation

$$E = E^0 + (RT/nF)\ln[(I^*_{ESR} - I_{ESR})/I_{ESR}], \quad (1)$$

where R is the gas constant, T and F are the absolute temperature and the faradic constant and n is the electron number involved in the reaction; I_{ESR} and I^*_{ESR} are the ESR intensity and its maximum value recorded at the negative extreme of the potential region studied. It can be seen from

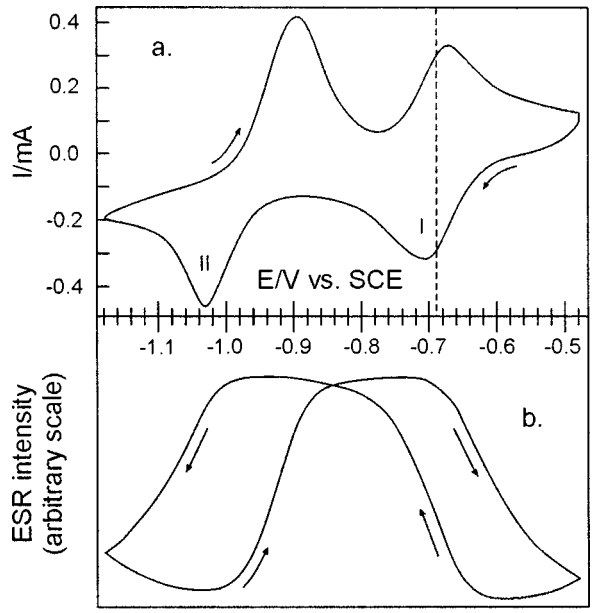

FIG. 7. SEESR measurements with a perforated Ag cylindrical electrode for 1 mmol/L MV+0.5 mol/L KCl aqueous solution, potential scan rate 10 mV/s. (a) Cyclic voltammetry; (b) ESR intensity as a function of potential.

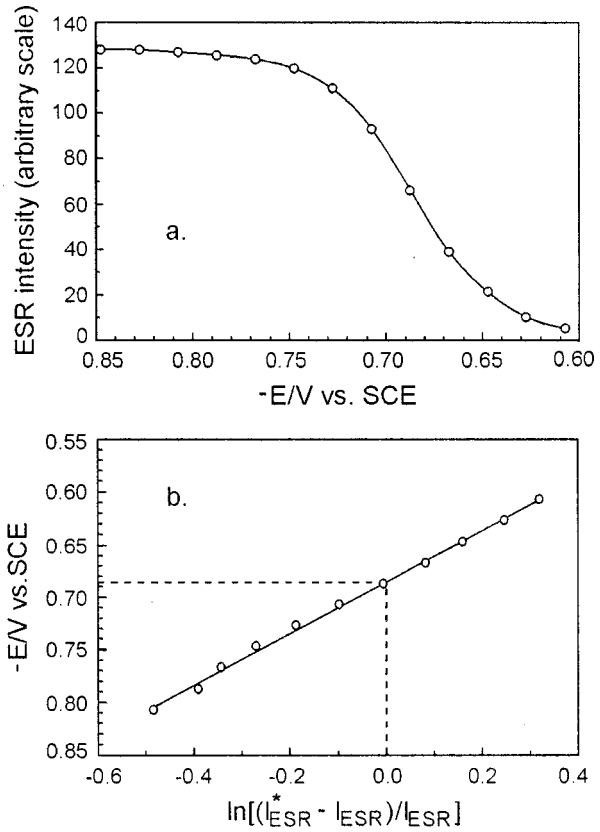

FIG. 8. Data of ESR thin-layer cell measurements with a cylindrical electrode for MV. (a) I_{ESR} vs E; (b) $\ln[(I^*_{ESR}-I_{ESR})/I^*_{ESR}]$ vs E.

Fig. 8(b) that there is a good linearity between $\ln[(I^*_{ESR} - I_{ESR})/I_{ESR}]$ and E, showing $n=1$ and $E^0 = -0.685$ V (versus SCE). These results are in good agreement with the characteristics of the cyclic voltammogram (Fig. 7) and the data reported in literature.[9]

E. Other applications

The cell designs reported in this article can be applied to a wide range of SEESR studies. Besides the demonstrative experiments described above, we have used perforated cylindrical electrode successfully to do potential modulated SEESR measurements[10] and to study conducting polymers.[11] In the work of potential modulated SEESR, the electrode was coated with Nafion. The electrode had to be cleaned mechanically after each measurement and reassembled for reuse. We found it much easier to clean and reuse the cylindrical electrode than a helix electrode. In another experiment, the SEESR measurements for the charge and discharge of lithiated carbons, the new design with a carbon-composite working electrode [Fig. 2(e)] was used successfully to replace the original sandwich design.[12] The latter is not suitable for study of the discharge process of lithiated carbon electrodes because the metallic lithium deposited at the counter electrode generates a huge interfering ESR signal.

ACKNOWLEDGMENT

The authors are grateful to the National Natural Science Foundation of China for financial support for this work.

[1] T. M. McKinney, *Electroanalytical Chemistry*, edited by A. J. Bard (Dekker, New York, 1965), Vol. 10, Chap. 2.
[2] B. Kastening, *Comprehensive Treatise of Electrochemistry*, edited by R. E. White, J. O'M Bockris, B. E. Conway, and E. Yeager (Plenum, New York, 1984), Chap. 7.
[3] I. B. Goldberg and T. M. McKinney, *Laboratory Techniques in Electroanalytical Chemistry*, edited by P. T. Kissinger and W. R. Heineman (Dekker, New York, 1996), Chap. 29.
[4] R. D. Allendoerfer, G. A. Martinchek, and S. Bruckenstein, Anal. Chem. **47**, 890 (1975).
[5] I. B. Goldberg and A. J. Bard, J. Phys. Chem. **75**, 3281 (1971).
[6] M. Sueki, G. A. Rinard, S. S. Eaton, and G. R. Eaton, J. Magn. Reson., Ser. A **103**, 208 (1993).
[7] T. Ogata, Y. Ishikawa, M. Ono, and L. J. Berliner, J. Mater. Res. **97**, 616 (1992).
[8] F. M. Hawkridge and T. Kuwana, Anal. Chem. **45**, 1021 (1973).
[9] C. L. Bird and A. T. Kuhn, Chem. Soc. Rev. **10**, 49 (1981).
[10] L. Zhuang and J. Lu, J. Electroanal. Chem. **429**, 115 (1997).
[11] S. Mu, J. Kan, J. Lu, and L. Zhuang, J. Electroanal. Chem. **446**, 107 (1998).
[12] L. Zhuang, J. Lu, X. Ai, and H. Yang, J. Electroanal. Chem. **397**, 315 (1995).